

# Laboratory activity 2: Digital position control of a DC servomotor (Theoretical background)

Riccardo Antonello\*

Francesco Ticozzi\*

April 14, 2025

## 1 Activity goal

The goal of this laboratory activity is to design a digital position controller for the DC servomotor available in the laboratory. Two different design approaches are considered: in the *design by emulation*, the digital controller is obtained by discretization of a controller that is originally designed in the continuous-time domain; vice versa, in the *direct digital design* (or *discrete design*), the control design is performed directly in the discrete-time domain, using a discrete-time model of the plant to be controlled.

## 2 Sampled-data control systems

A *sampled-data system* is a system where both continuous and discrete time signals coexist. A *sampled-data or digital control system* is a closed-loop control system where a continuous-time plant is controlled by a digital controller (see Fig 1).

The *digital controller* in Fig. 1 operates on the *samples*  $y[k]$ ,  $k \in \mathbb{Z}$  of the analog plant output  $y(t)$ ,  $t \in \mathbb{R}$ . The samples are collected at regularly spaced (under uniform sampling assumption) *sampling instants*  $t_k = kT$ ; the positive constant  $T$  is the *sampling period*, and  $f_s = 1/T$  is the *sampling frequency*. The sampling instants are provided by a *clock*.

The *analog-to-digital converter (ADC)* samples the continuous-time analog input  $y(t)$  at the sampling instants  $t_k$ , and converts the sampled values  $y(t_k)$  into binary numbers  $y[k]$  with a finite

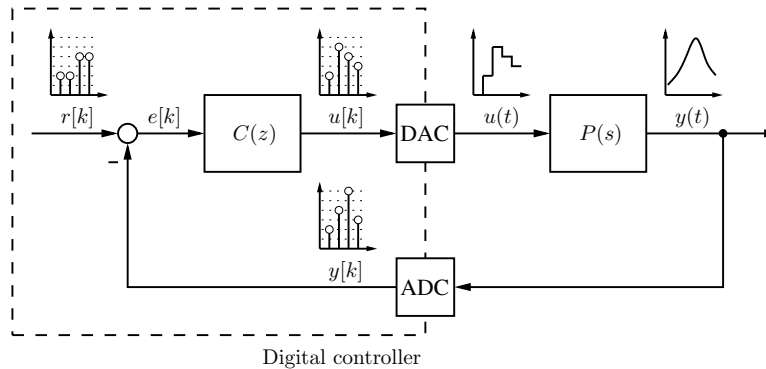


Figure 1: Sampled-data control system.

---

\*Dept. of Information Engineering (DEI), University of Padova; email: {antonello, ticozzi}@dei.unipd.it



Figure 2: Idealised elements for sampled-data system analysis: (a) ideal sampler; (b) zero-order holder (ZOH).

number of bits. The ADC output  $y[k]$  is a *digital signal*, i.e. it is a discrete-time, quantised-amplitude signal. The *digital-to-analog converter (DAC)* converts the digital signal  $u[k]$  (digital controller output) into an analog signal  $u(t)$ . The conversion usually consists of holding the input value  $u[k]$  over the whole *sampling interval*  $[kT, (k+1)T)$  (analog reconstruction based on *zero-order holding*). For the purpose of analysis and design, the ADC and DAC devices are replaced by their idealisations, namely the *ideal sampler* and the *(zero-order) holder (ZOH)*:

- *Ideal sampler*: it periodically samples the continuous-time analog input  $y(t)$  to yield the discrete time signal

$$y[k] = y(kT) \quad (1)$$

- *Zero-order holder*: it converts the discrete-time input signal  $u[k]$  into a continuous-time signal  $u(t)$  by holding it constant over the sampling intervals, i.e.

$$u(t) = u[k] \quad \text{for} \quad kT \leq t < (k+1)T \quad (2)$$

Note that the output  $y[k]$  of the ideal sampler and the input  $u[k]$  of the ZOH are not quantised in amplitude, i.e. they are not digital signals. Usually, a sampled-data system is regarded as an idealisation of a digital system, in which the amplitude quantisation of the digital signals is neglected. In a (single-rate) sample-data system, the ideal sampler and the ZOH are synchronised by the same clock: the ideal sampler instantaneously samples its input, and the ZOH output instantaneously jumps at the sampling instants.

### 3 Analysis of a sampled-data control system

There are fundamentally two alternative methods for analysing a sampled-data control system:

- analysis in continuous-time domain*: the series of the ideal sampler, the discrete-time controller and the ZOH (see Fig. 8) is described with an *approximate* continuous-time model.
- analysis in discrete-time domain*: the series of the ZOH, the continuous-time plant and the ideal sampler (see Fig. 3b) is described with an *approximate* discrete-time model.

#### 3.1 Analysis of a sampled-data control system in the continuous-time domain

The analysis in the continuous-time domain requires to define suitable continuous-time models of the ideal sampler and the ZOH, before deriving a continuous-time model of the sampled-data controller.

### 3.1.1 Continuous-time model of the ideal sampler

A continuous-time model of the ideal sampler is the *impulsive sampler*, which is defined as a modulator with a train of Dirac impulses as the *carrier signal*, and the analog input to be sampled as the *modulating signal*. Let the carrier signal be defined as

$$\delta_T(t) = \sum_{k=-\infty}^{+\infty} \delta(t - kT) \quad (3)$$

Then the output of the impulsive sampler is (reminding the *revealing property* of the Dirac impulse, which states that  $y(t) \delta(t - t_0) = y(t_0) \delta(t - t_0)$ )

$$y^*(t) = y(t) \delta_T(t) = \sum_{k=-\infty}^{+\infty} y(kT) \delta(t - kT) \quad (4)$$

Note that both  $y(t)$  and  $y^*(t)$  are continuous-time signals. For the analysis of the sampled-data system, it is required to relate the Laplace ( $\mathcal{L}$ ) and Fourier ( $\mathcal{F}$ ) transforms

$$Y(s) = \mathcal{L}\{y(t)\}(s), \quad Y(j\omega) = \mathcal{F}\{y(t)\}(\omega) \quad (5)$$

of the impulsively sampled signal  $y^*(t)$  with:

- the  $\mathcal{L}$  and  $\mathcal{F}$  transforms

$$Y(s) = \mathcal{L}\{y(t)\}(s), \quad Y(j\omega) = \mathcal{F}\{y(t)\}(\omega) \quad (6)$$

of the analog input  $y(t)$ .

- the Zeta ( $\mathcal{Z}$ ) and Discrete-Time Fourier Transform (DTFT)

$$\bar{Y}(z) = \mathcal{Z}\{\bar{y}[k]\}(z), \quad \bar{Y}(e^{j\omega T}) = \mathcal{F}\{\bar{y}[k]\}(\omega) \quad (7)$$

of the discrete-time signal<sup>1</sup>  $\bar{y}[k] = y(kT)$ .

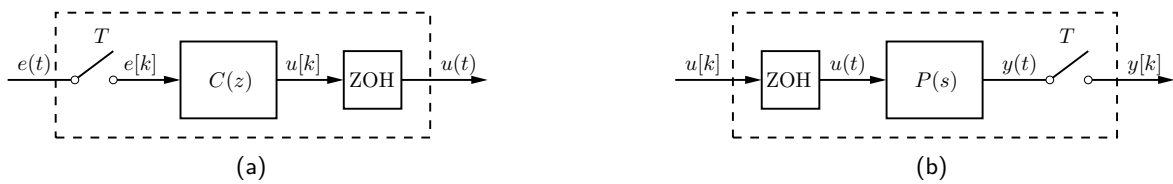


Figure 3: Analysis of a sampled-data control system: (a) sampled-data controller; (b) sampled-data plant.

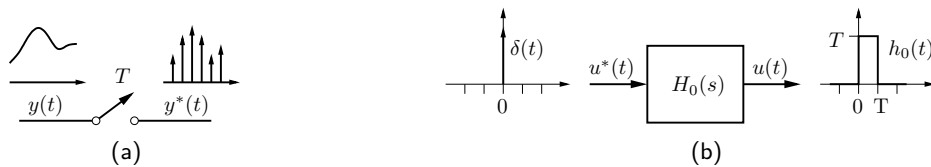


Figure 4: Continuous-time models of the ideal sampler and the ZOH: (a) impulsive sampler; (b) continuous-time model of the ZOH.

<sup>1</sup>The definition of the new symbol  $\bar{y}[k]$  in place of the original  $y[k]$  is required in the following to avoid ambiguity

The following relationships can be established:

a) relationship between  $Y(s)$  and  $Y^*(s)$ : the impulse train signal  $\delta_T(t)$  is periodic, so that it can be decomposed into a Fourier series:

$$\delta_T(t) = \sum_{n=-\infty}^{+\infty} c_n e^{jn\omega_s t} \quad \text{with} \quad c_n = \frac{1}{T} \int_{-T/2}^{T/2} \delta_T(t) e^{-jn\omega_s t} dt = \frac{1}{T} \quad (8)$$

where  $\omega_s = 2\pi f_s$  is the sampling frequency in [rad/s] units. Then, from (4) it follows that

$$Y^*(s) = \mathcal{L}\{y^*(t)\}(s) = \frac{1}{T} \sum_{n=-\infty}^{+\infty} \mathcal{L}\{y(t)e^{jn\omega_s t}\}(s) = \frac{1}{T} \sum_{n=-\infty}^{+\infty} Y(s - jn\omega_s) \quad (9)$$

b) relationship between  $Y^*(s)$  and  $\bar{Y}(z)$ : by applying the definition of the Laplace transform to the impulsively sampled signal (4), it follows that

$$\begin{aligned} Y^*(s) &= \mathcal{L}\{y^*(t)\}(s) = \int_0^{+\infty} y^*(t) e^{-st} dt = \int_0^{+\infty} \sum_{n=-\infty}^{+\infty} y(t) \delta(t - nT) e^{-st} dt \\ &\dots = \sum_{n=0}^{+\infty} y(nT) e^{-snT} = \sum_{n=0}^{+\infty} \bar{y}[n] (e^{sT})^{-n} = \bar{Y}(z) \Big|_{z=e^{sT}} \end{aligned} \quad (10)$$

namely the  $\mathcal{L}$ -transform of  $y^*(t)$  coincides with the  $\mathcal{Z}$ -transform of  $\bar{y}[k]$  evaluated at  $z = e^{sT}$ . In particular, the map  $z = e^{sT}$  establishes a connection between the  $s$ -plane of the Laplace transform and the  $z$ -plane of the  $\mathcal{Z}$ -transform.

c) relationship between  $Y^*(j\omega)$ ,  $\bar{Y}(e^{j\omega T})$  and  $Y(j\omega)$ : by setting  $s = j\omega$  in (9), and by using (10), it follows that:

$$Y^*(j\omega) = \bar{Y}(e^{j\omega T}) = \frac{1}{T} \sum_{n=-\infty}^{+\infty} Y(j(\omega - n\omega_s)) \quad (11)$$

In particular,  $Y^*(j\omega)$  is obtained as the sum of infinitely many replicas of  $Y(j\omega)$ , that are frequency shifted by multiples of  $\omega_s$ . The relationship (11) admits the graphical representation reported in Fig. 5. Assume that the continuous-time signal  $y(t)$  has the band-limited spectrum  $Y(j\omega)$  shown in Fig. 5a, whose support is the interval  $[-\omega_B, \omega_B]$ . For graphical convenience, assume that  $Y(j\omega) \in \mathbb{R}$  (in general, the spectrum is a complex value quantity, i.e.  $Y(j\omega) \in \mathbb{C}$ ). Let  $\omega_N = \omega_s/2$  denotes the *Nyquist frequency*. If the signal band  $\omega_B$  is smaller than the Nyquist frequency, i.e.  $\omega_B < \omega_N$ , then the spectrum of the sampled signal is as shown in Fig. 5b, in which the frequency-shifted replicas of  $Y(j\omega)$  do not overlap. On the other hand, if the signal band  $\omega_B$  is larger than the Nyquist frequency, i.e.  $\omega_B > \omega_N$ , then adjacent frequency-shifted replicas of  $Y(j\omega)$  do overlap, giving rise to the so called *aliasing phenomenon*. Reconstruction of the original continuous-time signal from the sampled one is possible only when the aliasing phenomenon does not occur, as stated by the *Shannon's sampling theorem*.

---

in notation between the  $\mathcal{L}$ -transform of  $y(t)$  and the  $\mathcal{Z}$ -transform of  $y[k]$

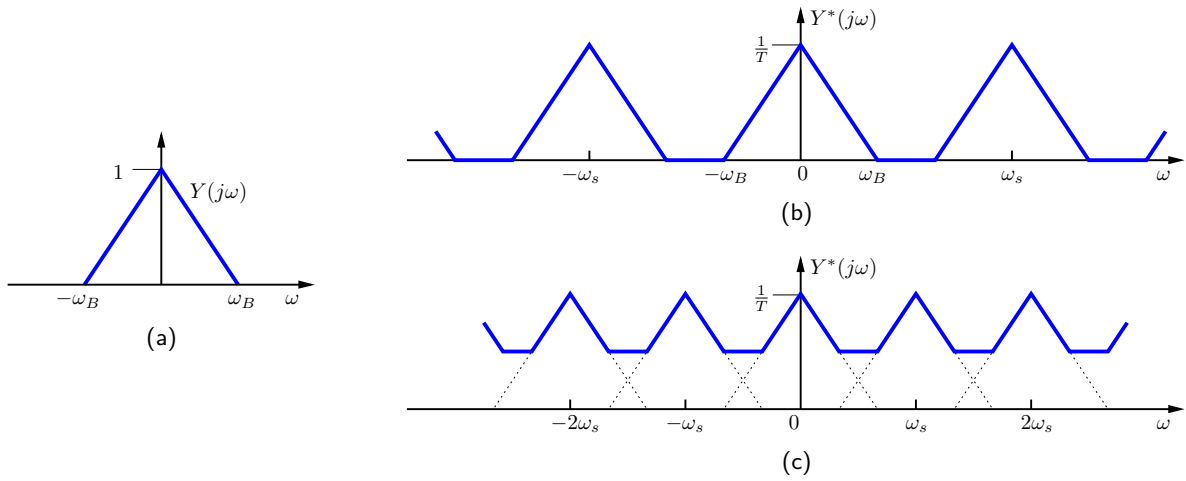


Figure 5: Graphical interpretation of the spectrum of a sampled signal: (a) spectrum of the original band-limited signal; (b) spectrum of the sampled signal when  $\omega_B < \omega_s/2$ ; (c) spectrum of the sampled signal when  $\omega_B > \omega_s/2$  (*aliasing phenomenon*).

**Theorem** (*Shannon's sampling theorem*).

Let  $y(t)$  be a continuous-time signal with a band-limited spectrum, i.e.  $|Y(j\omega)| = 0$  for  $|\omega| > \omega_B$ . If

$$\omega_B < \omega_N \quad (12)$$

with  $\omega_N = \omega_s/2 = \pi/T$  denoting the *Nyquist frequency*, the signal  $y(t)$  can be exactly reconstructed from the (impulsively) sampled signal  $y^*(t)$ . The reconstruction can be performed by filtering  $y^*(t)$  with a “brick-wall” low-pass filter (also known as *sinc-filter*) of the type:

$$H(j\omega) = \begin{cases} T & -\omega_N \leq \omega \leq \omega_N \\ 0 & \text{otherwise} \end{cases} \quad (13)$$

□

The reconstruction process with a “brick-wall” low-pass filter is graphically depicted in Fig. 6.

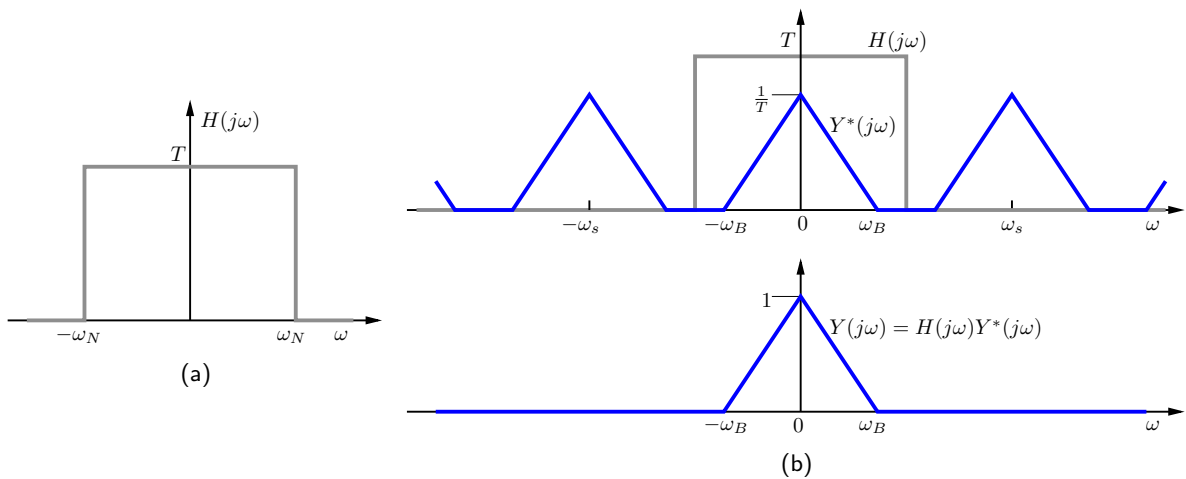


Figure 6: Reconstruction of a continuous-time signal from its sampled version (satisfying the conditions of the Shannon's sampling theorem): (a) reconstruction filter; (b) reconstruction process.

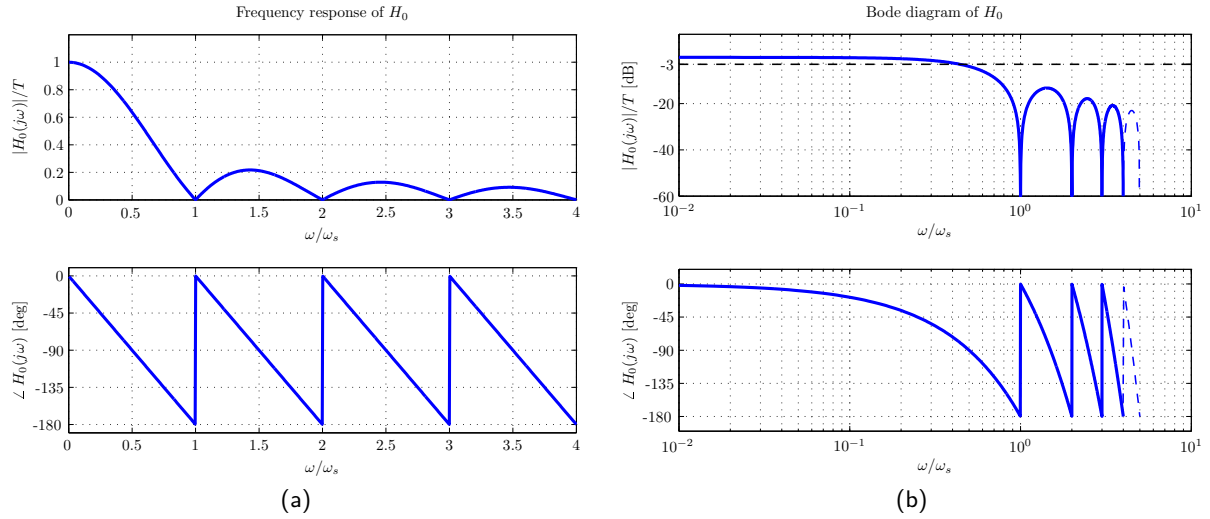


Figure 7: Frequency response of the filter  $H_0(s)$ : (a) linear scale plot; (b) logarithmic scale plot (Bode plot).

### 3.1.2 Continuous-time model of the zero-order holder

A continuous-time model of the ZOH can be obtained by replacing the discrete-time input  $u[k]$  with its impulsively sampled version  $u^*(t)$ . After replacing  $u[k]$  with  $u^*(t)$ , the ZOH can be modelled as a continuous-time filter with impulse response  $h_0(t)$  given by (see also Fig. 4b):

$$h_0(t) = \delta_{-1}(t) - \delta_{-1}(t - T) \quad (14)$$

where  $\delta_{-1}(t)$  denotes the unit step, applied at the origin. The transfer function is

$$H_0(s) = \mathcal{L}\{h_0(t)\}(s) = \frac{1}{s} - \frac{e^{-sT}}{s} = \frac{1 - e^{-sT}}{s} \quad (15)$$

The frequency response is obtained by substituting  $s = j\omega$  in the expression of the transfer function: it holds that

$$H_0(j\omega) = \frac{1 - e^{-j\omega T}}{j\omega} = e^{-j\omega T/2} \frac{e^{j\omega T/2} - e^{-j\omega T/2}}{j\omega} = T e^{-j\omega T/2} \frac{\sin(\omega T/2)}{\omega T/2} \quad (16)$$

The frequency response is shown in Fig. 7, both in linear and logarithmic (Bode plot) scales.

### 3.1.3 Continuous-time model of the sampled-data controller

Consider the sampled-data controller shown in Fig. 8a, consisting of the series of the ideal sampler, the discrete-time controller and the ZOH. A continuous-time model is obtained by first replacing the discrete-time output  $\bar{u}[k]$  with its impulsively sampled version  $u^*(t)$ , and the ZOH with the filter  $H_0(s)$  defined in Sec. 3.1.2. Then, by using (10), it follows that

$$U(z) = C(z) E(z) \implies U^*(s) = C(e^{sT}) E^*(s) \quad (17)$$

$$U^*(s) = \bar{U}(e^{sT})$$

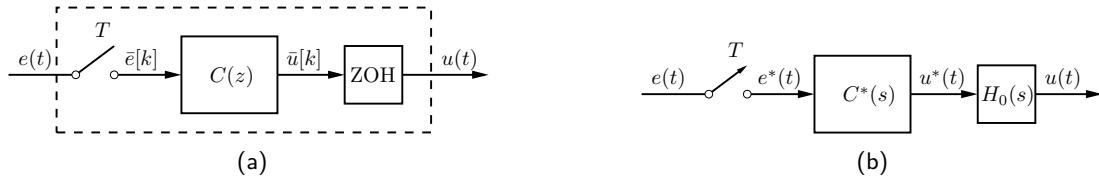


Figure 8: Continuous-time model of a sampled-data controller: (a) original controller; (b) continuous-time model.

Define  $C^*(s) = C(e^{sT})$ ; then, the continuous-time model of the sampled-data controller is as shown in Fig. 8b. The transfer function from the continuous-time input  $E(t)$  to the continuous-time output  $U(t)$  is

$$U(s) = H_0(s) C^*(s) E^*(s) \quad \text{with} \quad E^*(s) = \frac{1}{T} \sum_{n=-\infty}^{+\infty} E(s - jn\omega_s) \quad (18)$$

By setting  $s = j\omega$  in (18) it follows that

$$U(j\omega) = H_0(j\omega) C^*(j\omega) E^*(j\omega) \quad \text{with} \quad E^*(j\omega) = \frac{1}{T} \sum_{n=-\infty}^{+\infty} E(j(\omega - n\omega_s)) \quad (19)$$

If the input  $e$  is band-limited, with bandwidth  $\omega_B < \omega_N$ , then the following approximation can be introduced:

$$E^*(j\omega) H_0(j\omega) \approx \frac{1}{T} E(j\omega) H_0(j\omega) \quad \forall \omega \in [0, +\infty) \quad (20)$$

The approximation is valid because  $H_0(s)$  is a low-pass filter with cut-off frequency smaller than  $\omega_N$ , and therefore all the frequency-shifted replicas of  $E(j\omega)$  beyond the Nyquist frequency are well attenuated. By using the approximation (20) in (19) it follows that

$$U(j\omega) \approx \frac{1}{T} H_0(j\omega) C^*(j\omega) E(j\omega) \quad \text{for} \quad \omega \in [0, +\infty) \quad (21)$$

Moreover, by noting that

$$H_0(j\omega) \approx T e^{-j\omega T/2} \quad \text{for} \quad |\omega| \leq \omega_N \quad (22)$$

the expression (21) can be further reduced to

$$U(j\omega) \approx e^{-j\omega T/2} C^*(j\omega) E(j\omega) \quad \text{for} \quad \omega \in [0, \omega_N) \quad (23)$$

Therefore, under the hypothesis of a band-limited input signal  $e$ , with bandwidth  $\omega_B < \omega_N$ , the frequency response of the continuous-time model is

$$\frac{U(j\omega)}{E(j\omega)} \approx \frac{1}{T} H_0(j\omega) C^*(j\omega) \quad \text{for} \quad \omega \in [0, +\infty) \quad (24)$$

or

$$\frac{U(j\omega)}{E(j\omega)} \approx e^{-j\omega T/2} C^*(j\omega) \quad \text{for} \quad \omega \in [0, \omega_N) \quad (25)$$

where  $C^*(j\omega) = C(e^{j\omega T})$ . By using the the substitution  $s = j\omega$  in (24), the following transfer function for the continuous-time model can be immediately obtained

$$\frac{U(s)}{E(s)} \approx \frac{1}{T} H_0(s) C^*(s) \quad \text{where} \quad C^*(s) = C(e^{sT}) \quad (26)$$

### 3.2 Analysis of a sampled-data control system in the discrete-time domain

The analysis in the discrete-time domain requires to define a suitable discrete-time model of the series connection of the ZOH, the plant and the ideal sampler (sampled-data plant, see Fig. 3b).

Let  $\Sigma = (\mathbf{A}, \mathbf{B}, \mathbf{C}, \mathbf{D})$  be a state-space model of the plant <sup>2</sup>. By using the *Lagrange's formula*

$$\mathbf{x}(t) = e^{\mathbf{A}(t-t_0)} \mathbf{x}(t_0) + \int_{t_0}^t e^{\mathbf{A}(t-\tau)} \mathbf{B} u(\tau) d\tau \quad (27)$$

with  $t_0 = kT$  and  $t = (k+1)T$ , it follows that

$$\mathbf{x}((k+1)T) = e^{\mathbf{A}T} \mathbf{x}(kT) + \int_{kT}^{(k+1)T} e^{\mathbf{A}[(k+1)T-\tau]} \mathbf{B} u(\tau) d\tau \quad (28)$$

Because of the presence of the ZOH, the input  $u(\tau)$  is constant and equal to  $u[k]$  when  $\tau \in [kT, (k+1)T)$ . Therefore

$$\begin{aligned} \mathbf{x}((k+1)T) &= e^{\mathbf{A}T} \mathbf{x}(kT) + \left[ \int_{kT}^{(k+1)T} e^{\mathbf{A}[(k+1)T-\tau]} \mathbf{B} d\tau \right] u(kT) \\ &= \underbrace{e^{\mathbf{A}T}}_{\triangleq \mathbf{\Phi}} \mathbf{x}(kT) + \underbrace{\left[ \int_0^T e^{\mathbf{A}\eta} \mathbf{B} d\eta \right]}_{\triangleq \mathbf{\Gamma}} u(kT) \end{aligned} \quad (29)$$

which yields the discrete-time plant model

$$\begin{cases} \mathbf{x}[k+1] = \mathbf{\Phi} \mathbf{x}[k] + \mathbf{\Gamma} u[k] \\ y[k] = \mathbf{C} \mathbf{x}[k] + \mathbf{D} u[k] \end{cases} \quad (30)$$

whose input-output transfer function from  $u[k]$  to  $y[k]$  is equal to

$$P(z) = \mathbf{C} (z\mathbf{I} - \mathbf{\Phi})^{-1} \mathbf{\Gamma} + \mathbf{D} \quad (31)$$

There is a strict relationship between the eigenvalues of the original continuous-time plant model and its discretised version, which is summarised in the following fact.

**Fact** (*Relationship between continuous and discrete time plant eigenvalues*).

The eigenvalues  $s_i \in \mathbb{C}$ ,  $i = 1, \dots, n$  of  $\mathbf{A}$  are related to the eigenvalues  $z_i \in \mathbb{C}$  of  $\mathbf{\Phi} = e^{\mathbf{A}T}$  by the relation:

$$z_i = e^{s_i T} \quad i = 1, \dots, n \quad (32)$$

In particular:

---

<sup>2</sup>A SISO plant is considered in the following: however, the analysis reported in this section can be immediately extended, without any particular change, to the MIMO case.



1. the imaginary axis  $s = j\omega$  is mapped into the unit circle  $|z| = 1$
2. the point  $s = 0$  is mapped into the point  $z = 1$
3. the LHP in the  $s$ -plane is mapped into the region within the unit circle in the  $z$ -plane

□

The proof of (32) is immediate, since if  $\lambda \in \mathbb{C}$  is an eigenvalue of the matrix  $A$  with associated eigenvector  $v$ , then  $e^{\lambda t}$  is an eigenvalue of the matrix exponential  $e^{At}$  with the same associated eigenvector  $v$ . By using the transformation  $z = e^{sT}$ , it is possible to determine how the specific regions of the  $s$ -plane are mapped into the  $z$ -plane. The interesting regions are:

a) region of eigenvalues associated with system modes having a decaying ratio faster than the exponential  $e^{\sigma_0 t}$ , namely the region

$$S_\sigma = \{s = \sigma + j\omega \in \mathbb{C} : \sigma < \sigma_0, \omega \in \mathbb{R}\} \quad (33)$$

The region  $S_\sigma$  and its corresponding region in the  $z$ -plane are shown in Fig. 10a.

b) region of eigenvalues having a damping ratio greater than  $\delta_0$ , namely

$$S_\delta = \{s = -\delta \omega_n \pm j\omega_n \sqrt{1 - \delta^2} \in \mathbb{C} : 0 \leq \delta \leq \delta_0 < 1, \omega_n > 0\} \quad (34)$$

The region  $S_\delta$  and its corresponding region in the  $z$ -plane are shown in Fig. 10b.

c) region of eigenvalues having a natural frequency smaller than  $\omega_{n0}$ , namely

$$S_\omega = \{s = -\delta \omega_n \pm j\omega_n \sqrt{1 - \delta^2} \in \mathbb{C} : 0 \leq \delta \leq 1, 0 \leq \omega_n \leq \omega_{n0}\} \quad (35)$$

The region  $S_\delta$  and its corresponding region in the  $z$ -plane are shown in Fig. 10c.

It is worth to notice that the map  $z = e^{sT}$  from the  $s$ -plane to the  $z$ -plane is not bijective: in fact, given  $s_0 \in \mathbb{C}$ , the points  $s = s_0 + jk\frac{2\pi}{T}$  are mapped into the same point in the  $z$ -plane. This is equivalent to say that stripe regions of height  $2\pi/T$  in the  $s$ -plane are mapped into the interior or the exterior of the unit disc in the  $z$ -plane, depending on whether the stripe extends in the left or right half part of the  $s$ -plane. For stripes extending in the left-half complex plane, the correspondence with the interior of the unit disc in the  $z$ -plane is illustrated in Fig. 9. Note that the map  $z = e^{sT}$  becomes bijective when  $s \in \mathbb{C}$  is restricted to lie within a single horizontal stripe of height  $2\pi/T$  in the  $s$ -plane.

*Note:* according to the discretization procedure summarised in (27)–(30) (known as *exact* discretization method), a state-space model is required to obtain the discrete-time transfer function (31). An alternative method to obtain (31) without resorting to any state-space model is as follows. Consider to apply a unit discrete-time impulse  $u[k] = \delta[k]$  to the input of a sampled-data plant such as that shown in Fig. 3b. The output  $u(t)$  of the ZOH is

$$u(t) = \delta_{-1}(t) - \delta_{-1}(t - T) \quad (36)$$

whose  $\mathcal{L}$ -transform is equal to

$$U(s) = \mathcal{L}\{u(t)\}(s) = \frac{1 - e^{-sT}}{s} \quad (37)$$

The  $\mathcal{L}$ -transform of the plant output is

$$Y(s) = P(s)U(s) = P(s) \frac{1 - e^{-sT}}{s} \quad (38)$$

The time-domain response can be obtained by inverse  $\mathcal{L}$ -transformation, i.e.

$$y(t) = \mathcal{L}^{-1}\{P(s)U(s)\}(t) = \mathcal{L}^{-1}\left\{\frac{P(s)}{s}\right\}(t) - \mathcal{L}^{-1}\left\{\frac{P(s)}{s}\right\}(t - T) \quad (39)$$

The sampled version of (39), namely  $y[k] = y(kT)$ , is the discrete-time impulse response of the sampled-data plant: therefore, the  $\mathcal{Z}$ -transform of  $y[k]$  is the discrete-time transfer function of the sampled-data plant. It holds that:

$$\begin{aligned} P(z) &= \mathcal{Z}\{y[k]\}(z) \\ &= \mathcal{Z}\left\{\mathcal{L}^{-1}\left\{\frac{P(s)}{s}\right\}(kT) - \mathcal{L}^{-1}\left\{\frac{P(s)}{s}\right\}(kT - T)\right\}(z) \\ &= (1 - z^{-1}) \mathcal{Z}\left\{\mathcal{L}^{-1}\left\{\frac{P(s)}{s}\right\}(kT)\right\}(z) \end{aligned} \quad (40)$$

Introduce the definition

$$\mathcal{Z}\left\{\frac{P(s)}{s}\right\}(z) \triangleq \mathcal{Z}\left\{\mathcal{L}^{-1}\left\{\frac{P(s)}{s}\right\}(kT)\right\}(z) \quad (41)$$

which represents the  $\mathcal{Z}$ -transform of the sampled version of the unit step response of the continuous-time plant. Then, the transfer function (40) can be rewritten as follows

$$P(z) = (1 - z^{-1}) \mathcal{Z}\left\{\frac{P(s)}{s}\right\}(z) \quad (42)$$

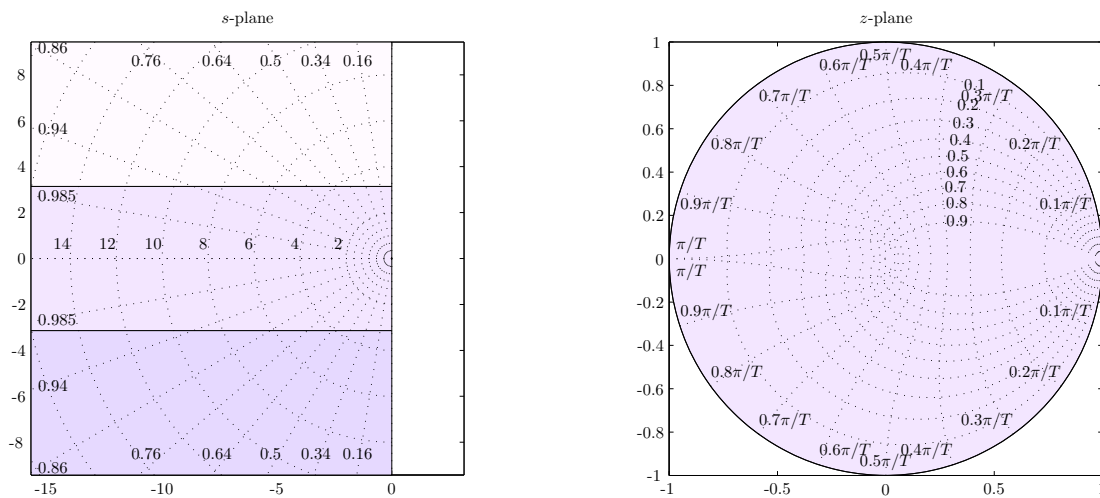
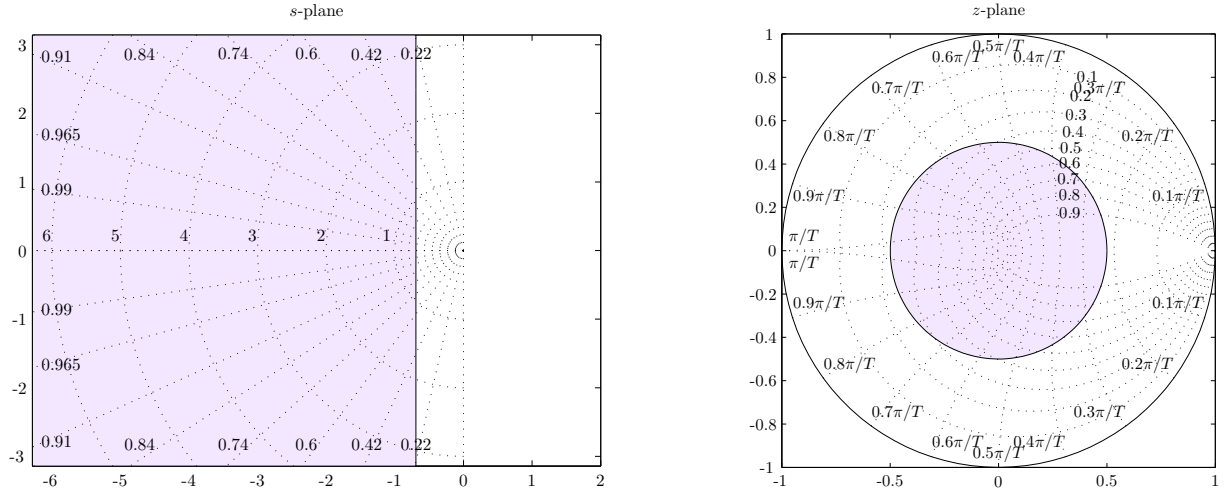
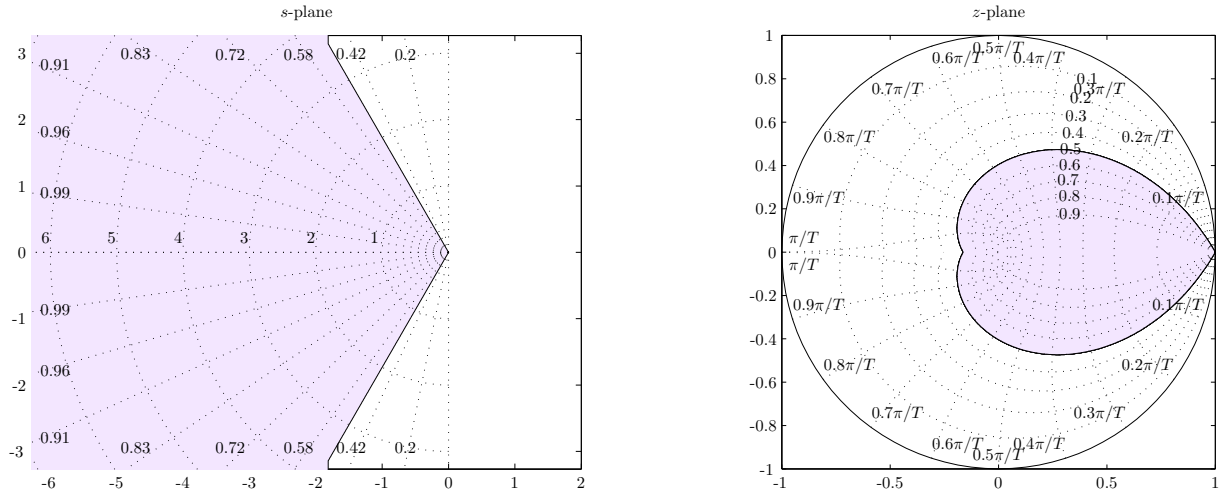


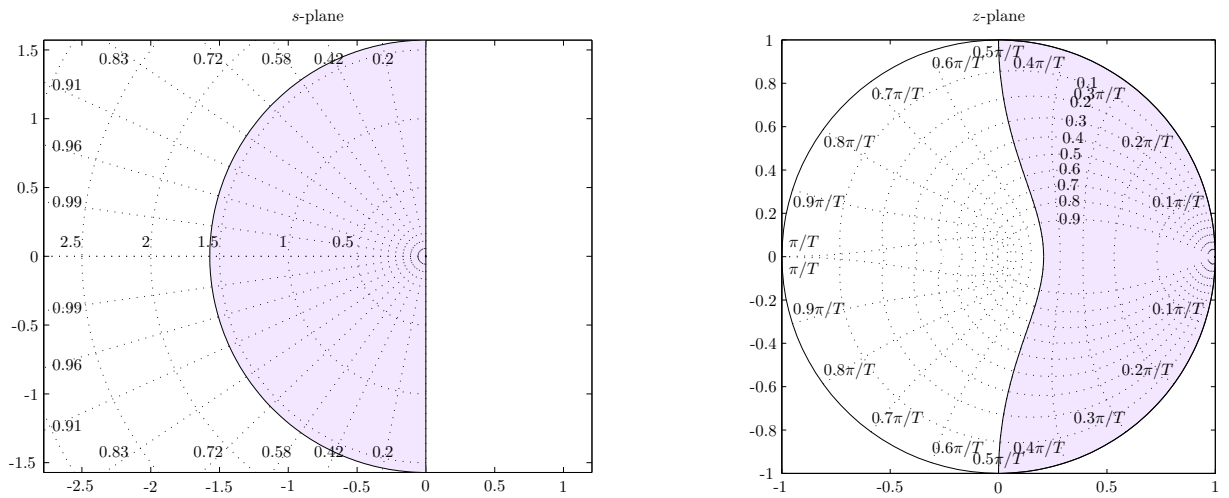
Figure 9: Non-bijection of the transformation  $z = e^{sT}$ .



(a) Eigenvalues with system modes decaying faster than  $e^{\sigma_0 t}$ .



(b) Eigenvalues with damping ratio greater than  $\delta_0$ .



(c) Eigenvalues with natural frequency smaller than  $\omega_{n0}$ .

Figure 10: Correspondences between the  $s$  and  $z$  planes, according to the transformation  $z = e^{sT}$ .

which is another way (alternative to (31)) of expressing the discrete-time transfer function of the sampled-data plant depicted in Fig. 3b. Differently from (31), note that no plant state-space model is required to evaluate (42): indeed, the only information required in this case is the plant transfer function  $P(s)$  or, alternatively, the plant unit step response  $\mathcal{L}^{-1}\{P(s)/s\}(t)$ .

## 4 Design of a sampled-data control system

There are fundamentally two alternative methods for designing a sampled-data control system:

a) *design in continuous-time domain (design by emulation)*: the control design is performed in the continuous-time domain, using either classical design methods (e.g. Bode's method, root locus method, etc.) or modern design methods (e.g. state-space methods).

Then, a discrete-time controller approximating the response of the original continuous-time controller is obtained by applying a *discretization procedure*.

b) *design in discrete-time domain (direct digital design, or discrete design)*: the control design is performed directly in the discrete-time domain, after obtaining a discrete-time model of the plant to be controlled with the methods explained in Sec. 3.2 (*exact* discretization of the continuous-time plant model).

### 4.1 Design by emulation

Say  $C_0(s)$  the transfer function of the controller designed in continuous-time domain using either classical or modern design methods. The *discretization problem* consists of finding a discrete-time controller  $C(z)$  such that the input-output transfer function of the sampled-data controller shown in Fig. 8, say  $D(s)$ , approximates (in some sense) the transfer function  $C_0(s)$ .

If the input  $e(t)$  satisfies the hypothesis of the sampling theorem, then, according to (26), the transfer function of the sampled-data controller is

$$D(s) = \frac{1}{T} H_0(s) C^*(s) = \frac{1}{T} H_0(s) C(e^{sT}) \quad (43)$$

In the frequency range  $[0, \omega_N)$  it holds that:

$$D(s) \approx e^{-sT/2} C(e^{sT})$$

In order to have  $D(s) \approx C_0(s)$ , it is necessary that:

$$e^{-sT/2} C(e^{sT}) \approx C_0(s) \quad \Rightarrow \quad C(e^{sT}) \approx e^{sT/2} C_0(s) \quad (44)$$

Therefore, a possible choice for the discretised controller  $C(z)$  is obtained from (44) by using the inverse of the transformation of  $z = e^{sT}$ , namely  $s = (1/T) \log z$ . It follows that

$$C(z) = e^{sT/2} C_0(s) \Big|_{s=\frac{1}{T} \log z} \quad (45)$$

The problem with the transfer function (45) is that it is not rational, even if  $C_0(s)$  is rational. Therefore, in order to overcome this issue, alternative discretization methods that produce rational transfer functions will be introduced in the following.

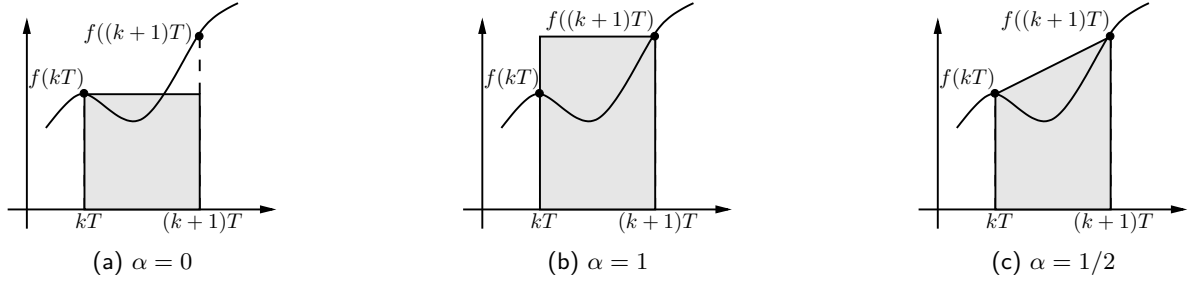


Figure 11: Discretization methods: (a) forward Euler method; (b) backward Euler method; (c) trapezoidal (Tustin's) method.

Let  $C_0(s)$  be the transfer function of the controller designed in the continuous-time domain, and  $\Sigma_C = (\mathbf{A}, \mathbf{B}, \mathbf{C}, \mathbf{D})$  a possible state-space realisation. Then, the equation of the state evolution

$$\dot{\mathbf{x}}(t) = \mathbf{f}(\mathbf{x}(t), e(t)) = \mathbf{A} \mathbf{x}(t) + \mathbf{B} e(t) \quad (46)$$

can be integrated to yield

$$\mathbf{x}((k+1)T) = \mathbf{x}(kT) + \int_{kT}^{(k+1)T} \mathbf{f}(\mathbf{x}(\tau), e(\tau)) d\tau \quad (47)$$

The following approximation can be introduced

$$\begin{aligned} \int_{kT}^{(k+1)T} \mathbf{f}(\mathbf{x}(\tau), e(\tau)) d\tau &\approx T [ (1-\alpha) \mathbf{f}(\mathbf{x}(kT), e(kT)) + \dots \\ &\dots + \alpha \mathbf{f}(\mathbf{x}((k+1)T), e((k+1)T)) ] \end{aligned} \quad (48)$$

where  $\alpha \in [0, 1]$ . The graphical interpretation of the approximation (48) is shown in Fig. 11, under the assumption of a scalar function  $\mathbf{f}$ . The approximation formula introduced above yields:

$$\mathbf{x}[k+1] - \mathbf{x}[k] = \mathbf{A} ( (1-\alpha) \mathbf{x}[k] + \alpha \mathbf{x}[k+1] ) T + \mathbf{B} ( (1-\alpha) e[k] + \alpha e[k+1] ) T \quad (49)$$

By applying the  $\mathcal{Z}$ -transform at both sides of the previous expression it follows that:

$$\left( \frac{1}{T} \frac{z-1}{\alpha z + 1 - \alpha} \mathbf{I} - \mathbf{A} \right) \mathbf{X}(z) = \mathbf{B} E(z) \quad (50)$$

By using the output equation  $u[k] = \mathbf{C} \mathbf{x}[k] + \mathbf{D} e[k]$ , it finally follows that:

$$C(z) = \frac{U(z)}{E(z)} = \mathbf{C} \left( \frac{1}{T} \frac{z-1}{\alpha z + 1 - \alpha} \mathbf{I} - \mathbf{A} \right)^{-1} \mathbf{B} + \mathbf{D} = C_0(s) \Big|_{s = \frac{1}{T} \frac{z-1}{\alpha z + 1 - \alpha}} \quad (51)$$

where the last identity holds because  $C_0(s) = \mathbf{C} (s\mathbf{I} - \mathbf{A})^{-1} + \mathbf{D}$ . The conclusion is that a discrete-time approximation of the continuous-time controller with transfer function  $C_0(s)$  is obtained by performing the substitution:

$$C_0(s) \xrightarrow[\text{Discretization}]{s = \frac{1}{T} \frac{z-1}{\alpha z + 1 - \alpha}} C(z) \quad (52)$$

Note that with the variable substitution reported in (52), the discretization of a rational continuous-

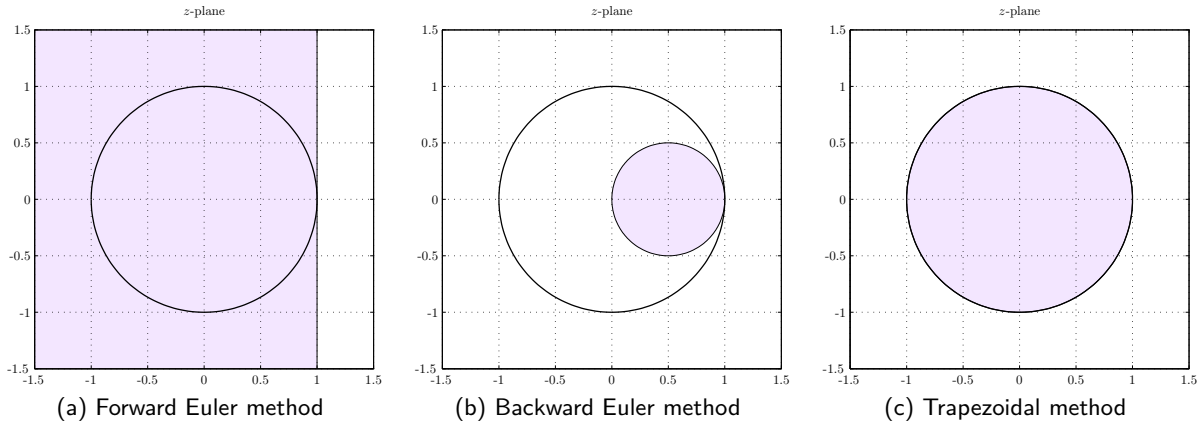


Figure 12: Mapping of the left-half  $s$ -plane onto the  $z$ -plane, with different discretization methods. The image of the left-half  $s$ -plane is highlighted with a shaded area.

time transfer-function  $C_0(s)$  is again a rational transfer function. Depending on the choice of  $\alpha$ , several discretization methods can be defined, as reported in Tab. 1. It is worth to notice that all

| Discretization method |                | Variable substitution                 |
|-----------------------|----------------|---------------------------------------|
| Forward Euler         | $\alpha = 0$   | $s = \frac{z - 1}{T}$                 |
| Backward Euler        | $\alpha = 1$   | $s = \frac{z - 1}{Tz}$                |
| Trapezoidal/Tustin    | $\alpha = 1/2$ | $s = \frac{2}{T} \frac{z - 1}{z + 1}$ |

Table 1: Discretization methods.

the variable substitutions defined in Tab. 1 are indeed rational approximations of the transformation  $z = e^{sT}$ , obtained by using the *Padé approximation* method. Depending on the variable substitution (and hence the discretization method) used, the left-half  $s$ -plane is mapped into different regions in the  $z$ -plane, as shown in Fig. 12. From the figure, it can be immediately noticed that not all the methods of Tab. 1 guarantee that the discretization of a stable continuous-time controller is still stable: in particular, the forward Euler method may produce an unstable discrete-time controller even if the original continuous-time one is stable.

Note: the discretization procedure illustrated in (52) applies to a controller described in terms of its transfer function. If the controller is specified in terms of a state-space model, then alternative discretization formulas can be derived from (49), which directly relate the state-space matrices of the continuous-time model to those of the discrete-time counterpart. These formulas are summarised in Tab 3. For completeness, the discretization formulas for a controller specified in terms of its transfer function are reported in Tab. 2.

## 4.2 Direct digital design

The direct design in the discrete-time domain can be performed with any of the available classical or modern design methods, after having obtained a discrete-time model of the plant to be controlled with the *exact* discretization method illustrated in Sec. 3.2.

| Forward Euler                 | Backward Euler                 | Trapezoidal                                 | Exact   |
|-------------------------------|--------------------------------|---|---|
| $C\left(\frac{z-1}{T}\right)$ | $C\left(\frac{z-1}{Tz}\right)$ | $C\left(\frac{2}{T} \frac{z-1}{z+1}\right)$ | $(1-z^{-1}) \mathcal{Z}\left\{\frac{C(s)}{s}\right\}$ |

Table 2: Discretization of a continuous-time transfer function  $C(s)$ .

|          | Forward Euler | Backward Euler         | Trapezoidal   | Exact                       |
|----------|---------------|------------------------|---|-----------------------------|
| $\Phi$   | $I + AT$      | $(I - AT)^{-1}$        | $\left(I + \frac{AT}{2}\right)\left(I - \frac{AT}{2}\right)^{-1}$ | $e^{AT}$                    |
| $\Gamma$ | $BT$          | $(I - AT)^{-1}BT$      | $\left(I - \frac{AT}{2}\right)^{-1}B\sqrt{T}$                     | $\int_0^T e^{A\tau}B d\tau$ |
| $H$      | $C$           | $C(I - AT)^{-1}$       | $\sqrt{T}C\left(I - \frac{AT}{2}\right)^{-1}$                     | $C$                         |
| $J$      | $D$           | $D + C(I - AT)^{-1}BT$ | $D + C\left(I - \frac{AT}{2}\right)^{-1}\frac{BT}{2}$             | $D$                         |

Table 3: Discretization of a continuous-time state-space model  $\Sigma_c = (A, B, C, D)$ .

## 5 Reduced-order state observers

An alternative to the use of a high-pass filter (i.e. “real derivative”) for estimating the motor speed from the position measurement consists of using a *state observer*. The main advantage of using an observer is that the speed signal can be potentially determined without the phase lag error that invariably affects the estimate provided by any high-pass filter. A *reduced-order state observer* can be used for the estimation of the motor speed, since the other state variable, namely the motor position, is directly measured with a sensor (e.g. optical encoder). The general design procedure for a reduced-order state observer is summarised in the following Sec. 5.1 (continuous-time case) and Sec. 5.2 (discrete-time case).

### 5.1 Continuous-time design

The design procedure for a generic continuous-time reduced-order state observer is articulated in the following steps:

- 1) Let  $\Sigma = (A, B, C, 0)$  be the state-space model of a continuous-time plant, whose state vector  $x \in \mathbb{R}^n$  has to be estimated. Assume that the model has  $m$  inputs and  $p$  outputs, and that  $\text{rank } C = p$ , i.e. all the plant outputs are linearly independent.

Consider the state transformation  $T$  such that

$$x' = T^{-1}x = \begin{bmatrix} C \\ V \end{bmatrix} = \begin{bmatrix} y \\ v \end{bmatrix} \quad (53)$$

where the  $n - p$  rows of  $V \in \mathbb{R}^{(n-p) \times p}$  are chosen to be linearly independent with the  $p$  rows of  $C$ . The vector  $v \in \mathbb{R}^{n-p}$  contains the unknown state variables to be estimated with the reduced-order state observer.

2) Rewrite the state model  $\Sigma$  in the new state variables  $\mathbf{x}' = \mathbf{T}^{-1}\mathbf{x}$ :

$$\Sigma' : \begin{cases} \dot{\mathbf{y}} = \mathbf{A}'_{11} \mathbf{y} + \mathbf{A}'_{12} \mathbf{v} + \mathbf{B}'_1 \mathbf{u} \\ \dot{\mathbf{v}} = \mathbf{A}'_{21} \mathbf{y} + \mathbf{A}'_{22} \mathbf{v} + \mathbf{B}'_2 \mathbf{u} \end{cases} \quad (54)$$

$$(55)$$

3) Define the known input/output quantities:

$$\bar{\mathbf{u}} \triangleq \mathbf{A}'_{21} \mathbf{y} + \mathbf{B}'_2 \mathbf{u} \quad (56)$$

$$\bar{\mathbf{y}} \triangleq \dot{\mathbf{y}} - \mathbf{A}'_{11} \mathbf{y} - \mathbf{B}'_1 \mathbf{u} \quad (57)$$

so that the state-space model  $\Sigma'$  becomes:

$$\Sigma' : \begin{cases} \dot{\bar{\mathbf{y}}} = \mathbf{A}'_{12} \mathbf{v} \\ \dot{\mathbf{v}} = \mathbf{A}'_{22} \mathbf{v} + \bar{\mathbf{u}} \end{cases} \quad (58)$$

$$(59)$$

which is a  $(n - p)$ -dimensional model with input  $\bar{\mathbf{u}}$  and output  $\bar{\mathbf{y}}$ .

4) Design a full-order state observer for estimating the state vector  $\mathbf{v} \in \mathbb{R}^{n-p}$  of  $\Sigma'$ , given the known input/output quantities  $\bar{\mathbf{u}}$  and  $\bar{\mathbf{y}}$ . The equation of the state observer dynamics is

$$\begin{aligned} \dot{\hat{\mathbf{v}}} &= \mathbf{A}'_{22} \hat{\mathbf{v}} + \bar{\mathbf{u}} + \mathbf{L} (\bar{\mathbf{y}} - \mathbf{A}'_{12} \hat{\mathbf{v}}) \\ &= (\mathbf{A}'_{22} - \mathbf{L} \mathbf{A}'_{12}) \hat{\mathbf{v}} + \underbrace{(\mathbf{A}'_{21} \mathbf{y} + \mathbf{B}'_2 \mathbf{u})}_{\equiv \bar{\mathbf{u}}} + \mathbf{L} \underbrace{(\dot{\mathbf{y}} - \mathbf{A}'_{11} \mathbf{y} - \mathbf{B}'_1 \mathbf{u})}_{\equiv \bar{\mathbf{y}}} \end{aligned} \quad (60)$$

5) To get rid of  $\dot{\mathbf{y}}$  in (60) (the computation of the ideal derivative is practically unfeasible), introduce the new variable  $\mathbf{z} \triangleq \hat{\mathbf{v}} - \mathbf{L} \mathbf{y}$ . Then

$$\dot{\mathbf{z}} = \dot{\hat{\mathbf{v}}} - \mathbf{L} \dot{\mathbf{y}} = (\mathbf{A}'_{22} - \mathbf{L} \mathbf{A}'_{12}) (\mathbf{z} + \mathbf{L} \mathbf{y}) + (\mathbf{A}'_{21} \mathbf{y} + \mathbf{B}'_2 \mathbf{u}) + \mathbf{L} (-\mathbf{A}'_{11} \mathbf{y} - \mathbf{B}'_1 \mathbf{u}) \quad (61)$$

After some computations, the equations of the reduced-order state observer become

$$\hat{\Sigma} : \begin{cases} \dot{\mathbf{z}} = \mathbf{A}_o \mathbf{z} + \mathbf{B}_o [\mathbf{u}, \mathbf{y}]^T \\ \hat{\mathbf{v}} = \mathbf{z} + \mathbf{L} \mathbf{y} \end{cases} \quad (62)$$

$$(63)$$

with

$$\begin{aligned} \mathbf{A}_o &= \mathbf{A}'_{22} - \mathbf{L} \mathbf{A}'_{12} \\ \mathbf{B}_o &= [\mathbf{B}'_2 - \mathbf{L} \mathbf{B}'_1, (\mathbf{A}'_{22} - \mathbf{L} \mathbf{A}'_{12}) \mathbf{L} + \mathbf{A}'_{21} - \mathbf{L} \mathbf{A}'_{11}] \end{aligned} \quad (64)$$

6) The estimate of the original state vector is given by

$$\hat{\mathbf{x}} = \mathbf{T} \hat{\mathbf{x}}' = \mathbf{T} \begin{bmatrix} \mathbf{y} \\ \hat{\mathbf{v}} \end{bmatrix} \quad (65)$$



Therefore, the equations of the reduced-order state observer in the original state variables are

$$\hat{\Sigma} : \begin{cases} \dot{\mathbf{z}} = \mathbf{A}_o \mathbf{z} + \mathbf{B}_o [\mathbf{u}, \mathbf{y}]^T \\ \hat{\mathbf{x}} = \mathbf{C}_o \mathbf{z} + \mathbf{D}_o [\mathbf{u}, \mathbf{y}]^T \end{cases} \quad (66)$$

$$(67)$$

with

$$\mathbf{C}_o = \mathbf{T} \begin{bmatrix} \mathbf{0}_{p \times (n-p)} \\ \mathbf{I}_{(n-p) \times (n-p)} \end{bmatrix}, \quad \mathbf{D}_o = \mathbf{T} \begin{bmatrix} \mathbf{0}_{p \times m} & \mathbf{I}_{p \times p} \\ \mathbf{0}_{(n-p) \times m} & \mathbf{L} \end{bmatrix} \quad (68)$$

The design of the reduced-order state observer consists of finding the gain matrix  $\mathbf{L} \in \mathbb{R}^{(n-p) \times p}$  such that the eigenvalues of  $\mathbf{A}_o = \mathbf{A}'_{22} - \mathbf{L} \mathbf{A}'_{12}$  are placed at certain desired locations in the open left-half complex plane. This corresponds to assign a prescribed rate of convergence of the estimation error  $\tilde{\mathbf{v}} = \mathbf{v} - \hat{\mathbf{v}}$  to zero, since this quantity is governed by the dynamical equation  $\dot{\tilde{\mathbf{v}}} = \mathbf{A}_o \tilde{\mathbf{v}}$ . The arbitrary placement of the observer eigenvalues is possible if and only if the pair  $(\mathbf{A}'_{22}, \mathbf{A}'_{12})$  is observable. It can be proved that a sufficient condition for the observability of the pair  $(\mathbf{A}'_{22}, \mathbf{A}'_{12})$  is that the pair  $(\mathbf{A}', \mathbf{C}')$  is observable or, alternatively, that the pair  $(\mathbf{A}, \mathbf{C})$  is observable, since observability is invariant for linear state transformations.

## 5.2 Discrete-time design

The design procedure for a discrete-time reduced-order observer is virtually identical to that of the continuous-time counterpart. Let  $\Sigma = (\Phi, \Gamma, \mathbf{H}, \mathbf{J})$  be the state-space model of a discrete-time plant, whose state vector  $\mathbf{x} \in \mathbb{R}^n$  has to be estimated. By following the procedure illustrated in Sec. 5.1 (with obvious adaptations for dealing with the discrete-time case), it can be easily verified that the discrete-time reduced-order state observer is described by the following equations:

$$\hat{\Sigma} : \begin{cases} \mathbf{z}[k+1] = \Phi_o \mathbf{z}[k] + \Gamma_o [\mathbf{u}[k], \mathbf{y}[k]]^T \\ \hat{\mathbf{x}}[k] = \mathbf{H}_o \mathbf{z}[k] + \mathbf{J}_o [\mathbf{u}[k], \mathbf{y}[k]]^T \end{cases} \quad (69)$$

$$(70)$$

with

$$\Phi_o = \Phi'_{22} - \mathbf{L} \Phi'_{12} \quad (71)$$

$$\Gamma_o = [\Gamma'_2 - \mathbf{L} \Gamma'_1, (\Phi'_{22} - \mathbf{L} \Phi'_{12}) \mathbf{L} + \Phi'_{21} - \mathbf{L} \Phi'_{11}]$$

and

$$\mathbf{H}_o = \mathbf{T} \begin{bmatrix} \mathbf{0}_{p \times (n-p)} \\ \mathbf{I}_{(n-p) \times (n-p)} \end{bmatrix}, \quad \mathbf{J}_o = \mathbf{T} \begin{bmatrix} \mathbf{0}_{p \times m} & \mathbf{I}_{p \times p} \\ \mathbf{0}_{(n-p) \times m} & \mathbf{L} \end{bmatrix} \quad (72)$$

where  $\mathbf{T}$  is the state transformation that partitions the state vector  $\mathbf{x}$  as specified in (53), and

$$\Phi' = \mathbf{T}^{-1} \Phi \mathbf{T} = \begin{bmatrix} \Phi'_{11} & \Phi'_{12} \\ \Phi'_{21} & \Phi'_{22} \end{bmatrix}, \quad \Gamma' = \mathbf{T}^{-1} \Gamma = \begin{bmatrix} \Gamma'_1 \\ \Gamma'_2 \end{bmatrix} \quad (73)$$